Acta Cryst. (1959). **12**, 465

The Crystal Structure of Hexagonal $CaAl_2Si_2O_8$

BY Y. TAKÉUCHI

Mineralogical Institute, Science Department, University of Tokyo, Hongo, Tokyo, Japan

AND GABRIELLE DONNAY

Geophysical Laboratory, Carnegie Institution of Washington, Washington, D.C., U.S.A.

(*Received* 29 *December* 1958)

The structure of hexagonal $CaAl_2Si_2O_8$ has been determined by two-dimensional Fourier methods. Double sheets of composition $Al_2Si_2O_8$ are made up of linked oxygen tetrahedra about (Si, Al) atoms. They are similar to the sheets found in hexagonal $BaAl_2Si_2O_8$, but are considerably deformed from hexagonal to trigonal symmetry, in such a way as to contract the cationic niches between the sheets. A comparison of the two structures illustrates the non-rigidity of the anionic layers.

Diffuse streaks on the Weissenberg photographs indicate mistakes in the stacking of the sheets. Such mistakes lead to the formation of trigonal prisms of oxygen atoms around calcium atoms, whereas in the ordered structure calcium is coordinated octahedrally. The Ca–O distance is found to be 2·39 Å in either coordination. The (Si, Al)–O distances are 1·66 and 1·71, both ±0·03 Å. The residual, $R = 13{\cdot}8\%$, refers to the 151 permitted non-equivalent reflections in the Cu $K\alpha$ sphere, 49 of which are structurally absent.

Introduction

In a previous note (Donnay, 1952) it was stated that hexagonal $CaAl_2Si_2O_8$ is not isostructural with low-temperature $BaAl_2Si_2O_8$ (Ito, 1950), although the cell geometry and space group are similar. Further study of the two polymorphic forms of the barium compound (Takéuchi, 1958) has shown that these forms differ in the detailed structure of their $Al_2Si_2O_8$ sheets; the low-temperature form has deformed six-membered rings within the sheets so that their symmetry is lowered from hexagonal to trigonal. As a result the coordination number of barium atoms, which lie between the sheets, is changed: it is reduced from 12 (in the high-temperature form) to 6. We suspected that the structure of $CaAl_2Si_2O_8$ might also contain distorted alumino–silicate sheets, distorted in such a way that the cation sites would be surrounded by the expected number of 6 oxygen atoms at reasonable calcium-to-oxygen distances. The structure analysis was undertaken in order to test this hypothesis.

Experimental procedure

The cell dimensions, obtained from precession films and refined from powder patterns (Donnay, 1952), are: $a = 5{\cdot}10 \pm 0{\cdot}01$, $c = 14{\cdot}72 \pm 0{\cdot}01$ Å. The cell contains two formula units, which leads to a calculated density of 2·78 g.cm.$^{-3}$, in agreement with the observed value of $2{\cdot}7 \pm 0{\cdot}1$ g.cm.$^{-3}$. The most probable space group was previously reported as $P6/mmm$ (former symbol $C6/mmm$ was used), with marked pseudo-halving of c. If, however, one accepts as significant the fact that, among the nine observed but very weak reflections with l odd, none is of the form $h0\bar{h}l$, the diffraction aspect is actually $P{*}c{*}$ and the most probable space group is D_{6h}^3–$P6_3/mcm$.

Equi-inclination Weissenberg films (multiple-film technique) were obtained with Cu $K\alpha$ radiation ($\lambda = 1{\cdot}5418$ Å). Intensites were estimated visually with an accuracy of about 10%; Lorentz and polarization corrections were applied. The crystal was small enough to justify neglecting absorption effects. Of the 151 independent permitted reflections in the Cu sphere, 49 were too weak to be observed. The relative values of $|F_o|$'s were put on an absolute scale in the course of the structure determination.

Structure analysis

Determination of x- and y-coordinates

With only two formula units per cell, the calcium atoms must occupy a two-fold position. Silicon and aluminum are each in a four-fold position, if they are not symmetrically equivalent; if they are equivalent, they may occupy an eight-fold position. Available positions for space group $P6_3/mcm$ are:

$n = 2$: (*a*) $(0, 0, \frac{1}{4})$; (*b*) $(0, 0, 0)$
$n = 4$: (*c*) $(\frac{1}{3}, \frac{2}{3}, \frac{1}{4})$; (*d*) $(\frac{1}{3}, \frac{2}{3}, 0)$; (*e*) $(0, 0, z)$
$n = 8$: (*h*) $(\frac{1}{3}, \frac{2}{3}, z)$.

Consideration of cell dimensions rules out position 4: (*e*) for silicon (or aluminum) atoms because it implies unreasonably short distances between Si (or Al) and Ca atoms. Thus, in a projection of the structure on (0001), the two Ca atoms must have coordinates (0, 0), while 2 (Si+Al) or 4 (Si, Al) will fall at $(\frac{1}{3}, \frac{2}{3})$ and $(\frac{2}{3}, \frac{1}{3})$. Only the coordinates of oxygen atoms must

be found. We therefore begin with the *c*-axis electron-density projection.

The arithmetic mean of f_{Si} and f_{Al} can, legitimately, be used in $F_{hk\cdot0}$ structure-factor calculations. Those $hk\cdot0$ reflections whose signs are determined with reasonable certainty by the metal atoms alone were used in the Fourier synthesis. Peaks are observed on the x axes at $x \simeq 0{\cdot}365$, indicating that the oxygen atoms O_{II} must occupy position (k), (x, 0, z), the only twelve-fold position that has $y = 0$. Of the sixteen oxygen atoms in the cell, the remaining four (O_I) must occupy position (c) or (d).

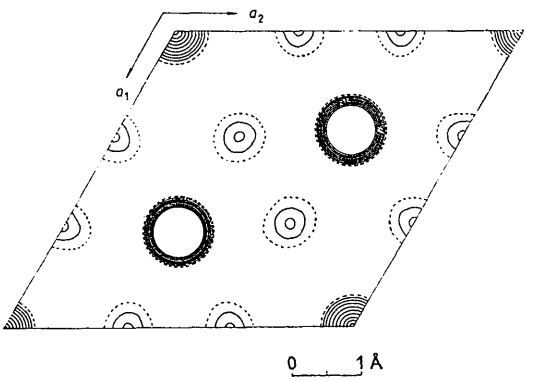

Fig. 1. Electron-density projection along the *c*-axis. Contours are drawn approximately at intervals of 5 e.Å^{-2}, the dotted contour being the zero-electron line. Contours in the central parts of the peaks at $\frac{1}{3}$, $\frac{2}{3}$ and $\frac{2}{3}$, $\frac{1}{3}$ are omitted.

The x-parameter of the oxygen position (k) was refined by means of a difference synthesis to the value of 0·370. It was confirmed by a final electron-density projection (Fig. 1). A residual R of 10·3% was obtained for all $hk\cdot0$ reflections. The atomic coordinates are listed in Table 1; the projection of the structure on (0001) is shown in Fig. 2.

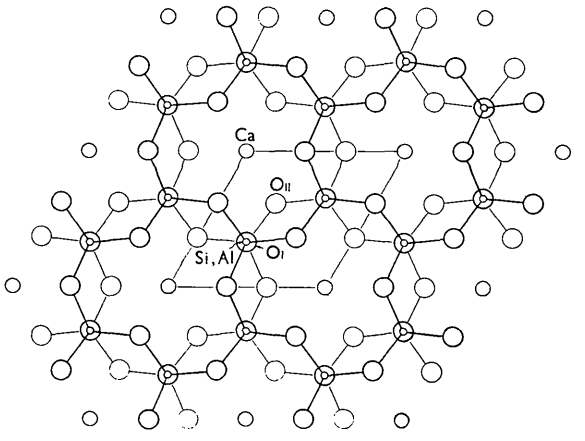

Fig. 2. Arrangement of atoms in the *c*-axis projection.

Table 1. *Atomic coordinates*

		x	y	z
2 Ca	at (b)	0	0	0
8 (Si, Al)	at (h)	$\frac{1}{3}$	$\frac{2}{3}$	$0{\cdot}137_5$
4 O_I	at (c)	$\frac{1}{3}$	$\frac{2}{3}$	$\frac{1}{4}$
12 O_{II}	at (k)	0·370	0	0·100

Determination of z-coordinates

A Patterson projection on ($1\bar{2}\cdot0$) was computed using $F^2_{h0\cdot l}$ reflections (Fig. 3(a)). All peaks appear on

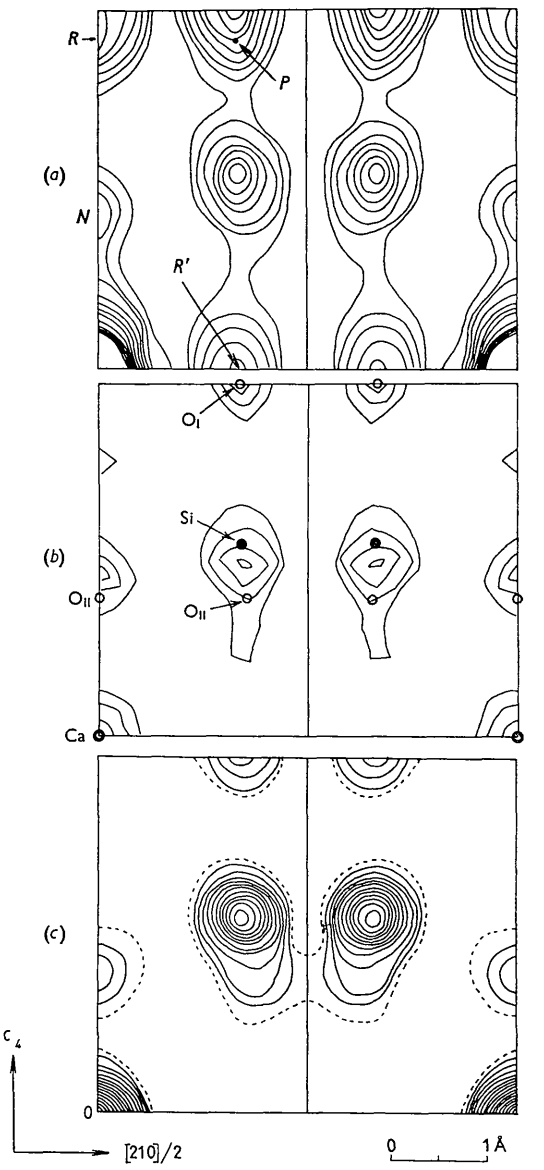

Fig. 3. (a) Patterson projection on ($1\bar{2}\cdot0$). (b) Minimum function $^{P,N}M_4(x, z)$ obtained from the above Patterson projection. The final positions of Si, (O_I and O_{II}), and Ca are indicated by solid circle, light open circle, and heavy open circle respectively. (c) Electron-density projection on ($1\bar{2}\cdot0$). Contours are drawn approximately at intervals of 2·5 e.Å^{-2}, the dotted contour being the zero-electron line.

Table 2. *Comparison of observed and calculated $F_{hk\cdot l}$'s corresponding to one formula unit*

$hk\cdot l$	$\|F_o\|$	F_c	$hk\cdot l$	$\|F_o\|$	F_c	$hk\cdot l$	$\|F_o\|$	F_c	$hk\cdot l$	$\|F_o\|$	F_c
00·0	—	138	20·4	14·2	16·4	50·6	2·4	−1·4	31·10	11·2	12·2
10·0	20·1	−15·4							31·12	9·6	9·8
20·0	4·5	−1·6	11·1	5·7	−8·2	11·2	13·3	−7·8	31·14	4·5	2·4
30·0	60·0	62·4	11·3	8·5	−11·5	11·4	6·1	2·7			
40·0	12·6	11·1	11·5	0	1·1	11·6	27·9	26·0	41·2	0	−0·9
50·0	5·3	3·3	11·7	6·5	8·1	11·8	34·5	36·2	41·4	8·1	−5·2
			11·9	<5	2·5	11·10	18·5	−23·3	41·6	16·1	14·3
11·0	47·4	47·6	11·11	<7	−4·1	11·12	7·4	−3·9	41·8	19·8	21·7
12·0	10·0	−9·2	11·13	<5	−3·3	11·14	31·3	28·4	41·10	10·4	−10·7
13·0	13·6	−11·6	11·15	0	1·3	11·16	17·8	16·7	51·2	7·6	8·5
14·0	23·2	22·9	21·1	<4	3·2	11·18	14·8	−13·5			
22·0	33·6	35·0	21·3	4·5	5·0	21·2	16·2	17·0	22·2	4·9	−3·3
23·0	6·2	8·4				21·4	19·9	20·0	22·4	7·6	−6·4
33·0	23·6	30·1	20·6	2·4	2·0	21·6	5·3	−2·0	22·6	14·3	17·7
			20·8	2·8	−4·1				22·8	25·3	28·3
00·2	11·2	9·6	20·10	22·7	24·1	21·5	0	−0·6	22·10	9·8	−14·4
00·4	35·0	−31·0	20·12	13·2	14·3	21·7	<5	−4·1	22·12	2·6	−2·5
00·6	6·5	−7·1	20·14	4·1	−3·4	21·9	0	−1·4	22·14	15·4	19·8
00·8	51·9	51·2				21·11	0	2·5	23·2	10·5	11·1
00·10	0	0·4	30·2	5·5	3·8	21·13	0	2·2	23·4	7·2	5·5
00·12	4·7	2·6	30·4	19·1	−23·9	21·15	0	−0·7	23·6	0	0·6
00·14	14·7	13·1	30·6	6·3	4·0	31·1	0	0·4	23·8	3·5	4·9
00·16	6·1	7·3	30·8	31·8	35·9	31·3	0	0·7	23·10	13·2	12·2
00·18	12·8	−10·1	30·10	4·5	−1·0	31·5	0	0·0	23·12	7·3	7·0
			30·12	3·1	2·2	31·7	0	−0·1	24·2	7·3	7·6
10·2	26·6	25·0	30·14	12·8	9·9				24·4	12·5	11·2
10·4	33·5	30·5	30·16	6·5	8·2	21·8	5·4	−4·1	24·6	6·5	7·6
10·6	13·9	12·0				21·10	17·3	18·0			
10·8	4·9	−6·5	40·2	10·0	10·2	21·12	9·5	11·3	31·9	0	0·2
10·10	18·3	20·2	40·4	17·3	18·7	21·14	0	−0·1	31·11	0	0·4
10·12	9·8	11·7	40·6	7·5	7·1	21·16	3·1	2·4	31·13	0	0·4
10·14	0	1·2	40·8	3·0	−4·3				41·1	0	−1·9
10·16	0	1·4	40·10	11·8	11·3	31·2	12·8	11·7	41·3	0	−2·7
10·18	14·8	13·9	40·12	7·7	8·1	31·4	19·4	18·6	41·5	0	0·4
			50·2	12·1	11·9	31·6	8·4	7·6	41·7	0	2·6
20·2	24·6	22·2	50·4	6·6	7·5	31·8	6·9	−5·0	41·9	0	0·9
									51·1	0	1·6

the lines $[0, z]$ and $[\frac{1}{3}, z]$, in agreement with the previously determined coordinates. When the plane group of the projection is *pmm*, as it is here, two reflection peaks, $R(u, 0)$ and $R(0, w)$ are associated with the rotation peak $P(u, w)$ in Patterson space (Buerger, 1951). It is, therefore, expected that the Patterson peak marked P (Fig. 3(*a*)), although not actually at the maximum position, will be a rotation peak because two reflection peaks marked R and R' are properly associated with it. A minimum function, ${}^{p}M_2(x, z)$, based upon the coordinates of this point was, therefore, prepared. Another minimum function ${}^{N}M_2(x, z)$ based upon a peak marked N was also considered. These two maps were then combined to give a map of a minimum function ${}^{pN}M_4/(x, z)$ shown in Fig. 3(*b*), which turns out to be very similar to the electron-density map $\varrho(x, z)$ of low-temperature (α)-hexagonal $BaAl_2Si_2O_8$ (Takéuchi, 1958). On the assumption that the present structure also contains $Al_2Si_2O_8$ sheets, approximate z-coordinates for all atoms could be obtained. Silicon and aluminum atoms have a z coordinate different from $\frac{1}{4}$ and 0; they must therefore be placed in position 8: (*h*) and, to be equivalent, must be in substitutional disorder. Using the arithmetic mean of their scattering factors is thus justified for all structure-factor calculations. The O_I atoms must lie on the mirror plane at $z = \frac{1}{4}$ in position 4: (*c*), and the z-parameter of O_{II} could be derived approximately from the known Si–O distance. Finally the calcium atoms must lie between the layers at $z = 0$ in position 2: (*b*). A difference synthesis led to the final z-parameters (Table 1), which gave a residual R of 11·6% for the $h0\cdot l$ reflections. The final a_2-axis electron-density projection is shown in Fig. 3(*c*); the atomic projection is shown in Fig. 4.

All remaining $F_{hk\cdot l}$'s were then calculated and compared with F_o's (Table 2). The R value, with structurally absent reflections taken into account, turns out to be 13·8%. Because the accuracy of the data is of that order of magnitude, no further refinement was attempted.

The only atoms that contribute to the structure factors of $hk\cdot l$ reflections with l odd are the oxygen atoms O_{II}; these reflections are accordingly very weak. On the Weissenberg photographs, the spots of reflections with small $\sin\theta$ are drawn out along the festoons of rows parallel to the c^*-axis (Fig. 5), and those with large $\sin\theta$ are hardly discernible. The observed peak intensities of these spots are therefore expected to be less than the calculated ones, which assume an ordered

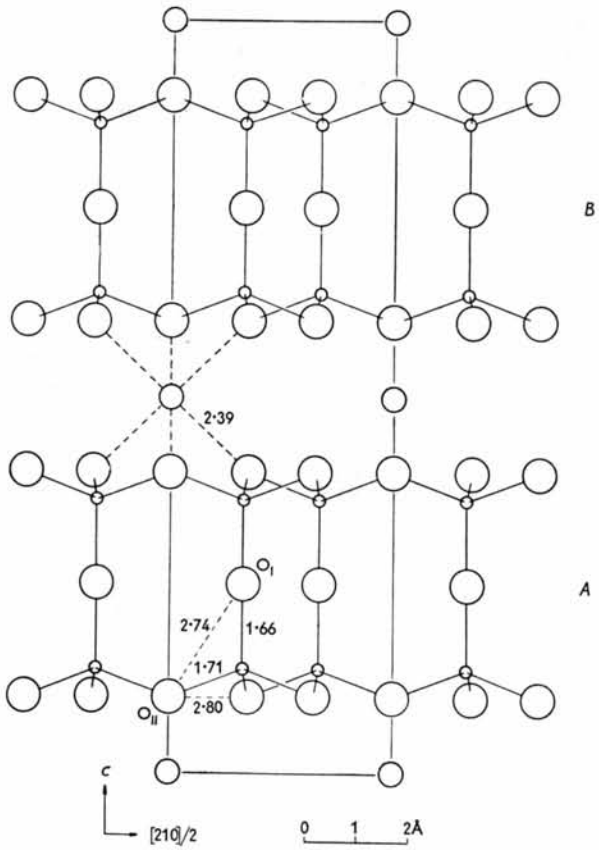

Fig. 4. Arrangement of atoms in the a_2-axis projection and interatomic distances.

structure. The expectation is borne out by the data (last section, Table 2). The interpretation of the diffuse peaks will be given below.

Discussion

Atomic distances and interbond angles

The termination error of the Fourier series was evaluated by calculating an F_c synthesis of the $(1\bar{2}\cdot0)$ electron-density projection. This gave a value slightly less than 0·03 Å for the probable error in the atomic distances between oxygen atoms O_{II}. In the a_2-axis projection, silicon–aluminum and oxygen atoms O_{II} are not well resolved. The z-coordinate of (Si, Al) seems, therefore, to be less accurate. As there was, however, very little drift in the coordinate of the (Si, Al) atom during refinement, it is not likely that the error of (Si, Al)–O distance exceeds the above value. Interatomic distances (given in Fig. 4) and their probable errors are listed in Table 3.

Table 3. *Interatomic distances*

Ca–O_{II}	2·39±0·02 Å
(Si, Al)–O_I	1·66±0·02
(Si, Al)–O_{II}	1·71±0·03
O_I–O_{II}	2·74±0·02
O_{II}–O_{II}	2·80±0·03

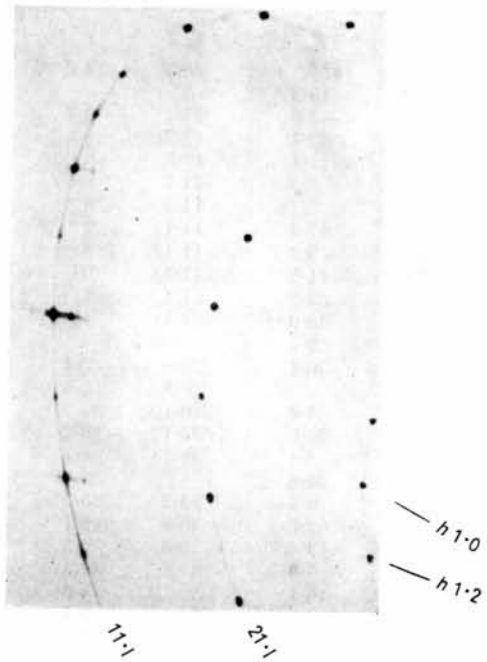

Fig. 5. Portion of Weissenberg photograph, a-axis, 1st layer, showing diffuse spots (Cu $K\alpha$, 35 kV., 15 mA., 12 hr.).

The mean value of (Si, Al)–O distances is $1{\cdot}68_5$ Å. The values derived from Goldschmidt's ionic radii are 1·60 Å and 1·76 Å for Si–O and Al–O distances respectively, giving a mean value of 1·68 Å, which agrees with the observed one. The bond angle (Si, Al)-O_{II}-(Si, Al) is equal to 119°; the angle of 180° found for (Si, Al)–O_I–(Si, Al) is unusual. It has previously been observed in sillimanite, Al_2SiO_5 (Taylor, 1928). Although sillimanite is usually considered an orthosilicate, it is possible, in its structure, to trace a compact chain of composition $Al_2Si_2O_{10}$ in which an Si–O–Al bond angle of 180° is found, as required by space-group symmetry. In hexagonal $CaAl_2Si_2O_8$ this angle may indicate that, owing to the high Al content, the (Si, Al)–O bond is more ionic than in the common silicates.

Structural disorder

The two $(Al_2Si_2)O_8$ sheets A and B (Figs. 4 and 6) contained in the cell are related to each other by a rotation of 180° followed by a translation of $c/2$. The stacking of these sheets in the ordered structure may be expressed by the sequence $ABABA\ldots$. Mistakes in the stacking sequence show up only in the positions of coplanar O_{II} atoms since this is the only feature in which the two layers differ. Even if the stacking of the layers were random, X-rays scattered by the O_{II} atoms are in phase for reflections $hk{\cdot}l$ with l even, and these reflections are accordingly normal; they are not in phase for $hk{\cdot}l$ with l odd, and these reflections are indeed observed to be diffuse.

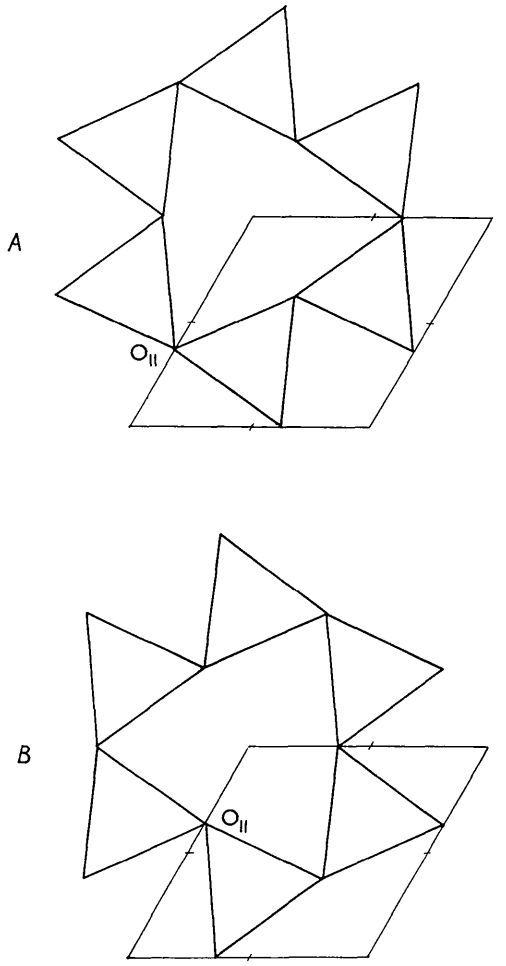

Fig. 6. The $(Al_2Si_2)O_8$ sheets with different orientations, *A* and *B*, in the cell of hexagonal $CaAl_2Si_2O_8$. Si, Al, and O_I atoms are not shown.

Mistakes in the stacking sequence change the coordination polyhedron about calcium, but leave the Ca–O distance equal to 2·39 Å and the coordination number equal to 6. The projection of the ordered structure along the a_2-axis (Fig. 4) shows the coordination polyhedron to be a trigonal antiprism, almost

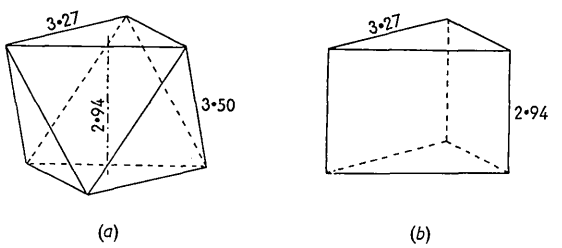

Fig. 7. Ca coordination polyhedra found in hexagonal $CaAl_2Si_2O_8$: (*a*) trigonal antiprism, (*b*) trigonal prism. Dimensions of the edges are given in Å units.

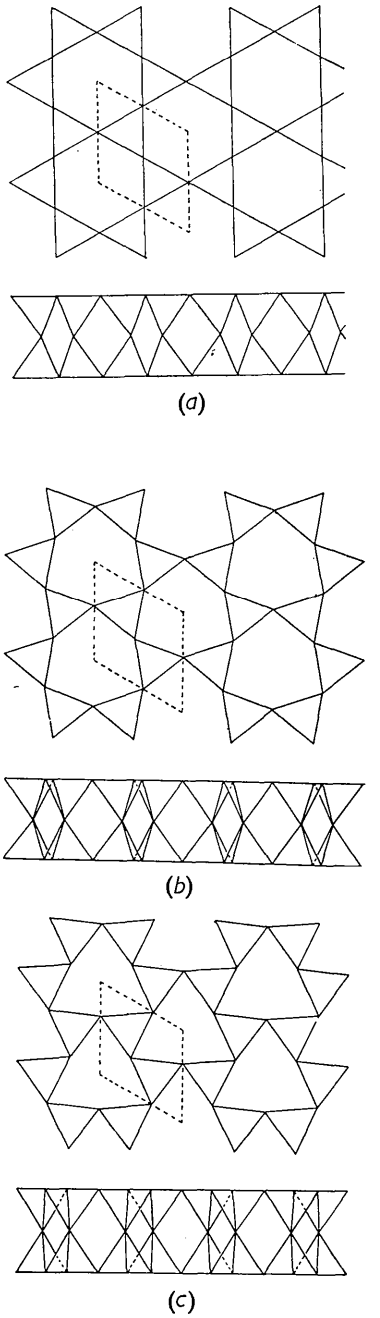

Fig. 8. $(Al_2Si_2)O_8$ sheets. In each case the upper diagram shows a view along the normal to the sheet (cell outlined by broken line), while the lower diagram gives a section viewed along the *a*-axis: (*a*) β-hexagonal $BaAl_2Si_2O_8$, (*b*) α-hexagonal $BaAl_2Si_2O_8$, (*c*) hexagonal $CaAl_2Si_2O_8$.

a regular octahedron (Fig. 7(*a*)), between layers *A* and *B*. It becomes a trigonal prism (Fig. 7(*b*)) between layers of the same kind; this polyhedron about calcium had been reported for apatite (Náray–Szabó, 1930).

Non-rigidity of (aluminum, silicon)–oxygen building blocks

The *c*-axis projection of the structure (Fig. 2) well illustrates one of its salient features—the sheet of composition $(Al_2Si_2)O_8$ in which each oxygen tetrahedron shares all its corners with neighboring tetrahedra, thus making the ratio O:(Si, Al) = 2:1. The degree of deformation from the ideal hexagonal symmetry of β-hexagonal $BaAl_2Si_2O_8$ (Fig. 8(*a*)) is much more pronounced in $CaAl_2Si_2O_8$ (Fig. 8(*c*)) than in α-hexagonal $BaAl_2Si_2O_8$ (Fig. 8(*b*)). It is therefore not surprising that no α–β transition has been observed for the calcium compound up to 1200 °C. (Davis & Tuttle, 1952). The solid solution (Ca, Ba)$Al_2Si_2O_8$ has not as yet been studied; it is expected to be either a complete series of solid solutions or one consisting of subphases related by high-order transitions as in the case of nepheline (Donnay *et al.*, 1959).

The non-rigidity of the oxygen tetrahedra in silicates is well illustrated by other structures in the literature. The $(Si_{2-n}Al_n)O_5$ sheets found in dickite by Newnham & Brindley (1956), in magnesium vermiculite by Mathieson (1954), and in monoclinic chlorite by Steinfink (1958) are all more or less deformed from the ideal hexagonal configuration. Hendricks & Jefferson, in their detailed work on the polymorphism of micas (1939), have suggested that in muscovite the mica sheets are considerably deformed from the ideal one given by Jackson & West (1930) but retain high symmetry in the biotites. They suggest that this state of affairs may be due to the difference in cations in the layers of oxygen octahedra. The recent publications on amphiboles by Whittaker (1949) and Zussman (1955) indicate similar phenomena.

The mineralogist cannot help but ask himself to what extent such structural changes in the (silicon, aluminum)–oxygen building blocks may occur within the solid-solution range of *one* mineral species. The example of nepheline (Na, K)$AlSiO_4$ has already been mentioned. Tourmaline, a mineral famous for its variable composition, may be another case in point. Two structures have been reported: they differ in the shape of the six-membered ring of tetrahedra. In (Al, Li)–tourmaline (Ito & Sadanaga, 1951), the ring has 6-fold symmetry; in Mg–tourmaline (Donnay & Buerger, 1950), it is ditrigonal. The magnesium and (aluminum, lithium) atoms occupy positions above the silicate ring and are octahedrally coordinated. The difference in their sizes may well be responsible for the difference in the two reported structures. In conclusion it may not be enough to carry out a careful structure determination on one crystal of a given composition. Instead of refining such a mineral structure in great detail we should perhaps study the structural changes which accompany changes in composition.

We are grateful to Prof. Ito and Dr R. Sadanaga for valuable comments, and to Prof. J. D. H. Donnay for a critical reading of the manuscript.

References

Buerger, M. J. (1951). *Acta Cryst.* **4**, 531.
Donnay, G. (1952). *Acta Cryst.* **5**, 153.
Donnay, G. & Buerger, M. J. (1950). *Acta Cryst.* **3**, 379.
Donnay, G., Schairer, J. F. & Donnay, J. D. H. (1959). *Min. Mag.* (In press).
Davis, G. L. & Tuttle, O. F. (1952). *Amer. J. Sci. Bowen volume*, p. 107.
Hendricks, S. B. & Jefferson, M. E. (1939). *Amer. Min.* **24**, 729.
Ito, T. (1950). *X-ray Studies on Polymorphism.* Tokyo: Maruzen.
Ito, T. & Sadanaga, R. (1951). *Acta Cryst.* **4**, 385.
Jackson, W. W. & West, J. (1930). *Z. Kristallogr.* **76**, 211.
Mathieson, A. McL. (1954). *Amer. Min.* **39**, 231.
Newnham, R. F. & Brindley, G. W. (1956). *Acta Cryst.* **9**, 759.
Náray-Szabó, St. (1930). *Z. Kristallogr.* **75**, 387.
Steinfink, H. (1958). *Acta Cryst.* **11**, 191.
Takéuchi, Y. (1958). *Mineralogical J.* (In press).
Taylor, W. H. (1928). *Z. Kristallogr.* **68**, 503.
Whittaker, E. J. W. (1949). *Acta Cryst.* **2**, 312.
Zussman, J. (1955). *Acta Cryst.* **8**, 301.